AD-A276 643

OFFICE OF NAVAL RESEARCH

Contract No. N00014-91-J-1409

Technical Report No. 148

The Adsorption of Sulfate on Gold(111) in Acidic Aqueous Media: Adlayer Structural Inferences from Infrared Spectroscopy and Scanning Tunneling Microscopy

by

Gregory J. Edens, Xiaoping Gao, and Michael J. Weaver

Prepared for Publication

in

Journal of Electroanalytical Chemistry

94-07828

DTIC ELECTE MAR 10 1994 S B D

Department of Chemistry

Purdue University

West Lafayette, Indiana 47907-1393

February 1994

Reproduction in whole, or in part, is permitted for any purpose of the United States Government.

* This document has been approved for public release and sale; its distribution is unlimited.

94 3 9 078 DTIC QUALITY INSPECTED 1

Best
Available
Copy

ABSTRACT

The potential-dependent adsorption of sulfate on ordered Au(111) from acidic aqueous electrolytes has been examined in-situ by means of infrared reflection-absorption spectroscopy (IRAS) and by atomic-resolution scanning microscopy (STM) in order to explore further the nature of the adsorbate bonding and the structural changes attending the formation of the ordered adlayer at high potentials, as observed recently by using STM (ref. 8). Solution conditions that encompassed aqueous sulfuric acid, sulfuric acid/sulfate electrolytes of varying pH, and dilute sulfate in excess perchloric acid were selected in order to facilitate comparisons with recent adsorbate compositional data extracted from chronocoulometric and radiotracer measurements which utilized the last type of electrolyte (ref. 9). Essentially the same ordered adlayer structures were deduced by STM to form at suitably high potentials ($\gtrsim$ 0.8 V vs. SCE) in both sulfuric acid and the mixed sulfate/excess perchloric acid media. The adlayer, which exhibits a ($\sqrt{3} \times \sqrt{7}$) symmetry, involves a fractional sulfate coverage of 0.2, in accordance with chronocoulometic and radiotracer data (ref. 9). The possibility that the ordered sulfate adlayer incorporates coadsorbed hydronium cations is discussed; such coadsorption is suggested by the presence of additional tunneling maxima in the STM images. The IRAS data display a prominent S-O stretching band (ν_{SO}) at 1155-1220 cm^{-1}, the potential-dependent intensity of which correlates with the sulfate surface concentrations reported in ref. 9. The appearance of this ν_{SO} feature is also insensitive to the electrolyte conditions, including pH, consistent with its assignment to adsorbed sulfate, rather than to bisulfate. The ν_{SO} frequency exhibits only a slight (ca 5 cm^{-1}) downshift upon forming the ordered adlayer, indicating that adsorbate ordering incurs no marked changes in the sulfate speciation or surface bonding.

Availability Codes
Dist | Avail and/or Special
A-1

INTRODUCTION

There are rapid advances currently being made in our understanding of adsorbate structure and bonding at ordered metal-solution interfaces. These developments are being fueled in large part by the emergence of an increasing swath of in-situ microscopic-level techniques (see ref. 1 for an overview). Perhaps most notably, scanning tunneling microscopy (STM) and synchrotron X-ray scattering techniques can now in suitable cases provide remarkably detailed spatial structural information for electrochemical adlayers as well as for the metal substrate[1-3]. For some polyatomic adsorbates, complementary in-situ information on surface bonding can also be obtained from infrared reflection-absorption spectroscopy (IRAS). The tandem application of STM and IRAS is therefore anticipated to provide a potent means of elucidating adlayer structure and bonding. We have recently utilized this STM/IRAS approach to deduce real-space adlayer structures, including adsorbate-substrate registries, for carbon monoxide on Rh(111)[4], Rh(110)[5], and Pt(111)[6], and cyanide on Pt(111)[7], all in aqueous media.

A distinctly different type of electrochemical adlayer which has also been characterized recently by in-situ STM involves anionic adsorption on Au(111) from aqueous sulfuric acid solutions[8]. Interestingly, an ordered structure was observed at high potentials which was assigned by Magnussen et al to a bisulfate adlayer having a fractional coverage of 0.4. A noteworthy feature of Au(111) and other gold surfaces is their near-ideal polarizable properties over wide potential ranges in aqueous media, enabling quantitative surface compositional data to be extracted from thermodynamic analyses of charge-potential measurements. Lipkowski and coworkers have undertaken such an analysis of sulfate/bisulfate adsorption on Au(111) from acidic mixed sulfate-perchlorate electrolytes by using chronocoulometric data[9]. They concluded on this basis

that sulfate (SO_4^{2-}), not bisulfate (HSO_4^-), was the predominant adsorbed species even for strongly acidic (pH ≈ 1) conditions. Moreover, the sulfate coverage, θ_{SO_4}, approached only about 0.2 at the highest potentials prior to Au(111) surface oxidation, where the ordered adlayer is apparently formed. The potential-dependent surface concentrations extracted from chronocoulometry were also found to be in good agreement with radiotracer measurements performed by Wieckowski et al[9].

The apparently disparate information provided by these STM[8] and surface compositional studies[9] have stimulated us to further examine sulfate/bisulfate adsorption on Au(111) by means of IRAS along with STM performed under electrolyte conditions that overlap with those employed in both refs. 8 and 9. The value of IRAS in this context stems from the anticipated sensitivity of the S-O vibrations to the nature and mode of surface binding of the sulfate/bisulfate adsorbate. Indeed, a number of in-situ IRAS examinations of sulfate/bisulfate adsorption have appeared recently, chiefly on platinum electrodes[10-19]. Claims of both predominant bisulfate or sulfate adsorption have been made in these studies, largely on the basis of the infrared data alone. Given the availability of quantitative surface composition data, it is of interest to examine the corresponding potential-dependent infrared spectra for sulfate adsorbed on Au(111). Furthermore, scrutinizing such spectra over an electrode potential range which encompasses the adsorbate disorder-order transition as sensed by STM should provide insight into the accompanying adsorbate structural changes.

Such IRAS data are reported in the present communication, along with corresponding atomic-resolution STM data obtained for the ordered Au(111)/sulfate adlayer using mixed sulfuric-perchloric acid electrolytes compatible with the thermodynamic analysis in ref. 9. When set alongside the surface compositional data, the IRAS and STM results lead us to consider a provocative structural

picture of sulfate adsorption on Au(111).

EXPERIMENTAL

The instrumentation and procedures for the electrochemical IRAS measurements have been described extensively elsewhere (e.g. refs. 20, 21). Briefly, the FTIR spectrometer was an IBM (Bruker) IR-98-4A instrument with a Globar source and a narrow-band MCT Detector. The spectroelectrochemical thin layer was formed by using a CaF_2 or ZnSe window. (While the former window material was found to be more inert in the presence of sulfuric acid, the latter yields markedly better infrared transmittance below 1100 cm^{-1}.) The surface spectra were obtained by utilizing the conventional potential-difference infrared (PDIR) tactic, involving coadding sets of interferograms acquired at a suitable ("reference" and "sample") pair of electrode potentials, the potential being alternated periodically (every 32 scans) to minimize spectral drift effects. A total of 500-1000 scans were typically acquired for each PDIR spectrum. The spectral resolution was 4 cm^{-1}.

The in-situ STM procedures are largely as described elsewhere[22,23]. The microscope is a Nanoscope II (Digital Instruments) with a bipotentiostat for electrochemical STM. The STM tips were iridium wires, sharpened by mechanical polishing and insulated with a thermosetting polyethylene plastic[23]. The counter electrode was a gold wire, and the quasi-reference electrode was an electrooxidized gold wire.

The Au(111) crystal used for both the IRAS and STM measurements was a 6 mm diameter hemisphere, prepared at CNRS, Meudon, France, by Dr. A. Hamelin. It was pretreated by flame annealing and cooled partly in air and then in ultrapure water[23], then transferred immediately to the IRAS or STM cell. All electrode potentials quoted here are versus the saturated calomel electrode (SCE).

RESULTS AND DISCUSSION

Infrared Spectra

Figure 1 shows a typical cyclic voltammogram obtained at 50 mV s^{-1} in the thin-layer IRAS cell for Au(111) in 0.1 M $HClO_4$ + 5 mM H_2SO_4 (solid trace). This mixed-electrolyte condition was chosen so to be compatible with that employed for the thermodynamic analysis in ref. 9 (vide infra). The asymmetry in the current-potential profiles between the positive- and negative-going potential sweeps arises partly from the iR drop in the thin-layer cell. Nonetheless, the broad capacitance feature centered around 0.5–0.6 V vs. SCE is a clear indication of sulfate specific adsorption[9]. The current spike seen at about 0.85 V signals the formation of the ordered sulfate adlayer towards higher potentials, as discerned from STM (vide infra)[8]. Also shown in Fig. 1 is a corresponding voltammogram obtained in 0.1 M H_2SO_4 (dashed trace), as employed for the STM data in ref. 8. Note that the voltammetric features for the dashed versus the solid trace are shifted slightly towards lower potentials, as expected given the higher sulfate/bisulfate concentration.

Series of PDIR spectra were acquired for these and other sulfate-containing acidic electrolytes for sequences of upper ("sample") potentials in the range of 0.4 to 1.2 V, where sulfate adsorption is encountered[9], with a fixed lower ("reference") potential of 0 V. The latter value was chosen in view of the negligible anion adsorption at this potential. Particular attention was paid to the potential region, 0.8–0.9 V, where the disorder–order transition is located. Figure 2A shows such a PDIR spectral set obtained in 0.1 M $HClO_4$ + 5 mM H_2SO_4. As already mentioned, this mixed-electrolyte condition with a large excess of a relatively nonadsorbing anion enables inner-layer surface excesses of sulfate, Γ_{SO4}, to be extracted directly from chronocoulometric data. Data involving a smaller sulfate concentration, 0.5 mM, were emphasized in ref. 9 to facilitate

overlap with the radiotracer data. For the present IRAS measurements, however, the slightly higher (5 mM) concentration is desirable to maintain an adequate quantity of anions in the thin-layer reservoir as are required for potential-induced adsorption (cf ref. 24).

The PDIR spectra in Fig. 2A show the presence of a single clearcut band centered at 1150-1220 cm^{-1}, the peak frequency, ν_{SO}, upshifting monotonically with increasing potential, E, as plotted in Fig. 3. The positive-going sign of this band, together with the ν_{SO}-E dependence, indicates that it is associated with adsorbed sulfate (or bisulfate). The integrated band intensity, A_1, reaches a maximum value towards the highest potentials. This is displayed in Fig. 4, where a plot of the average A_1 values obtained for 0.1 M $HClO_4$ + 5 mM H_2SO_4 (filled circles) versus E is compared with the corresponding Γ_{SO4}-E plot (open circles) extracted from chronocoulometric data for essentially the same electrolyte[9,25]. (We are grateful to Prof. J. Lipkowski for supplying the latter original data.) While the surface infrared band intensities are not necessarily precisely proportional to Γ_{SO4} (and hence θ_{SO4}), and absolute coverages are not readily obtainable by this means, the closely similar functionality evident in the A_1-E and Γ_{SO4}-E data argues strongly that the infrared band also arises from adsorbed sulfate anions. Supporting this conclusion is the observed similarity in the A_1-E dependence with the Γ_{SO4}-E plot (open triangles) extracted from radiotracer measurements[9], also shown in Fig. 3. While referring to a tenfold smaller sulfate concentration, the virtue of the radiotracer Γ_{SO4} values is that they extend to higher potentials than those obtainable from the chronocoulometric data. [This lower solution concentration accounts for the slightly smaller Γ_{SO4} values obtained by the radiotracer method (Fig. 3).]

A possible complication in interpreting PDIR spectra such as in Fig. 2A is that one would generally anticipate that the infrared features arising from

potential-induced adsorption would be accompanied by bands of opposite polarity associated with the removal of an equivalent quantity of solute from the thin-layer solution. The solution-phase and adsorbed band partners may interfere destructively if their frequencies are insufficiently different. This situation is in a sense most straightforward in the presence of an excess of supporting electrolyte, where an essentially fixed amount of adsorbing solute remains within the thin-layer cavity, the ion migration to and from the surrounding solution reservoir (required to balance the electronic charge flow) involving chiefly the supporting electrolyte[20,26,27]. Nonetheless, PDIR spectra obtained in the *absence* of supporting electrolyte may contain less interference from such solution-phase bands since the solute lost from the thin-layer solution by adsorption can be replenished by ion migration from the surrounding reservoir[26].

This latter condition is met in the potential-dependent sequence of PDIR spectra obtained for Au(111) in 0.1 M H_2SO_4, shown in Fig. 2B. The potential-dependent ν_{SO} frequencies and bandshapes for the ca 1150-1220 cm^{-1} feature seen in this electrolyte are seen to be very similar to those obtained in the mixed sulfate-perchloric acid medium (Fig. 2A), supporting the contention that solution-band spectral interferences are unimportant. A similar deduction was reached for sulfate/bisulfate adsorption on platinum by means of a flow-cell tactic[16]. If sulfate, rather than bisulfate, is indeed the predominant adsorbate even in such strongly acidic media, as appears to be the case[9], a negative-going band component at 1100 cm^{-1} would be expected on the basis of the solution transmittance spectra[28]. Such a weak feature was often observed in our spectra obtained in perchloric acid supporting electrolytes (also see below).

Two other aspects of the potential-dependent PDIR spectra are of particular significance in the present context. First, given the occurrence of a adlayer

disorder–order transition as seen directly by STM and signaled by the voltammetric spike at 0.8–0.9 V (Fig. 1), it is of interest to ascertain if any sharp changes in the ν_{SO} spectral fingerprint can be discerned at this point, which would be indicative of an alteration in the sulfate binding geometry and/or local environment. To this end, a number of spectral sequences were obtained at potentials close to (within 0.1 V of) the adlayer transition. Most of these measurements yielded a small (ca 5 cm^{-1}) yet noticeable downward-pointing inflection in the ν_{SO}–E dependence at the transition potential, suggesting that the formation of the ordered sulfate adlayer gives rise to a slightly lower ν_{SO} band frequency. This effect, however, is subtle enough to be barely evident in ν_{SO}–E plots spanning the full range of adsorption potentials (Fig. 3).

The other significant aspect of the present infrared spectral measurements concerns the band assignment. As already mentioned, the thermodynamic adsorption analysis in ref. 9 indicates that sulfate rather than bisulfate is the predominant adsorbate even for strongly acidic (pH ~ 1) conditions. While several authors have asserted that bisulfate (HSO_4^-) adsorption predominates instead on platinum in acidic media on the basis of band frequencies in comparison with solution species, assignments made on this basis alone are unconvincing since the nature of the ν_{SO} spectra will be sensitive to the mode of surface binding of the sulfate/bisulfate as well as to the presence or absence of a coordinated proton. This issue has been discussed by Nart and Iwasita[14,15], who point out that adsorbate infrared bands having frequencies well divorced from the corresponding solution-phase species will generally be expected as a result of symmetry lowering upon adsorption. While this factor can obfuscate band assignments, a worthwhile tactic is to examine the PDIR spectra over a range of pH values chosen so that the solution-phase concentration ratio, $[HSO_4^-]/[SO_4^{2-}]$, is markedly altered[15].

With this objective in mind, several sets of PDIR spectra were acquired for sulfate-containing electrolytes having pH values between 0.2 and 4, utilizing the ZnSe optical window so to facilitate detection of bands below 1100 cm^{-1}. Figure 5 shows a representative comparison between corresponding PDIR spectra obtained in 0.5 M H_2SO_4 (lower) and in 0.1 M Na_2SO_4 + 1 mM H_2SO_4 (upper spectrum). These electrolytes contain predominantly bisulfate and sulfate anions, respectively. The sample and reference potentials are 0.75 and 0 V, respectively. Both spectra show essentially the same positive-going band centered at ca 1190 cm^{-1}. In addition, a weak positive-going feature is also seen at 960 cm^{-1} in both spectra in Fig. 5 (cf Fig. 3). Similar spectral features are also obtained over the potential range ca 0.5-1.0 V. Both these bands are observed on Pt under mildly acidic conditions, and have been attributed to adsorbed SO_4^{2-}[15]. At low pH values on polycrystalline Pt, the ca 1200 cm^{-1} feature is attenuated, and replaced by an adsorbate band at ca 1100 cm^{-1}, which has been interpreted as anion adsorption occurring predominantly as bisulfate rather than sulfate[15]. The similar form of the positive-going bands on Au(111) as the H_2SO_4 concentration is varied (Fig. 5) therefore favors the occurrence of predominant sulfate adsorption even at low pH values in this system, in harmony with the deduction in ref. 9.

Nevertheless, an interesting difference between the pair of spectra shown in Fig. 5 is the presence of an additional *negative-going* feature at ca 1100 cm^{-1} in the higher pH electrolyte, which is absent in 0.5 M H_2SO_4. On the basis of the polarity and frequency of the band[15], it is assigned to the depletion of SO_4^{2-} in the thin-layer solution as the anion is adsorbed. This raises the question of why this feature is not also found for PDIR spectra in strongly acidic media, where the countercation is exclusively hydronium ions. A plausible explanation is that sulfate adsorption is accompanied by some cation

coadsorption, at least in the diffuse layer, so that there is a net depletion of HSO_4^- rather than SO_4^{2-} from the thin-layer solution when H_3O^+ is the sole electrolyte cation. In the higher pH electrolyte in Fig. 5, Na^+ rather than H_3O^+ is the predominant cation, so that SO_4^{2-} rather than HSO_4^- will be depleted from the thin-layer solution. We will return to this issue below.

The coordination geometry of the adsorbed sulfate can in principle also be deduced on the basis of the spectral patterns and group symmetry arguments. In practice, however, this procedure is quite ambiguous. Nart and Iwasita assigned the ca 1200 cm^{-1} and 950 cm^{-1} bands observed for sulfate on Pt to symmetric vibrations of SO_4^{2-} coordinated via two oxygens, yielding C_{2V} symmetry[15]. While this interpretation may well be correct, one can also envisage SO_4^{2-} binding occurring via one or even three oxygens; in each case the ν_{SO} band will split into several components upon oxygen coordination[30]. Indeed, the number of coordinated oxygens may increase with electrode potential: this can account both for the substantial ν_{SO} upshift (Fig. 3) and also the slight band narrowing observed under these conditions.

Scanning Tunneling Microscopy

The foregoing IRAS results show clearly that the nature and extent of sulfate adsorption, obtained in electrode potential regions corresponding to both disordered and ordered anion adlayers, is insensitive not only to the pH in acidic media, but also to the presence of the perchloric acid supporting electrolyte required for the thermodynamic assay of the inner-layer composition undertaken in ref. 9. Given that the published STM images for the ordered sulfate adlayer on Au(111) refer to 0.1 M or higher sulfuric acid concentrations[8], it was deemed desirable to obtain further STM data that encompass also the presence of perchloric acid electrolyte. Figure 6 shows a

representative STM image of a 12 nm square terrace region on Au(111) in 0.1 M $HClO_4$ + 5 mM H_2SO_4. The lower portion of the (upward-rastered) image was obtained at a potential, 0.5 V, where the adsorbed sulfate is sufficiently mobile so that the Au(111) substrate structure is evident from the characteristic hexagonal packing of the gold atoms, spaced 0.29 nm apart. About one-third up the image, the potential was stepped to 0.9 V, i.e. beyond the voltammetric spike (Fig. 1). An ordered adlayer is seen to be formed almost immediately ($\lesssim$ 0.5 s), as evidenced from the sudden marked change in the imaged pattern. The adlayer row directions with respect to the underlying gold lattice can be ascertained accurately in such "mixed-domain images" by mutually extrapolating the adlayer and substrate patterns into each other (cf refs. 2, 29). The more densely packed adlayer rows were ascertained in this manner to lie along the $\sqrt{3}$ direction, i.e. bisecting the gold substrate rows. The less densely spaced adlayer rows are seen to lie along the $\sqrt{7}$ direction, i.e. at an angle of 19° (and 41°) to the substrate rows. Given also that the interatomic spacing along these rows are $\sqrt{3}$ (0.50 nm) and $\sqrt{7}$ (0.76 nm), we can assign a ($\sqrt{3} \times \sqrt{7}$) unit cell to the structure. This unit cell, more properly described as $\begin{pmatrix} 2 & 1 \\ 1 & 2 \end{pmatrix}$, is in harmony with the observations of Magnussen et al[8]. In principle, mixed-domain images such as Fig. 6 can also yield the adlayer-substrate registry, i.e. the binding site geometry[2,29]. While this procedure is less straightforward on densely packed (111) planes than on more corrugated [e.g. (110)] surfaces, we deduce the adsorbate to be located at atop sites, possibly by binding oxygens to adjacent multifold sites.

Images containing the ($\sqrt{3} \times \sqrt{7}$) unit cell were reproducibly observed at potentials above the voltammetric spike for a range of sulfuric acid concentrations at least down to 5 mM, in both the absence and presence of perchloric acid supporting electrolyte. Depending on the tunneling conditions, however, STM images could be obtained that feature an additional tunneling

maximum within each unit cell. An example of such an image obtained at 0.9 V in 0.1 M H_2SO_4 is shown in Fig. 7 (in a 30° off-normal height-shaded representation). Along with the main tunneling maxima, again forming a ($\sqrt{3} \times \sqrt{7}$) unit cell, an equal number of nearby weaker maxima are also discernable. [These "satellite spots" do not result from "double-tip" imaging or related artifacts, as can be discerned from the appearance of mixed-domain images[8], and the occasional (yet clear) observation of single-atom defects interrupting such ($\sqrt{3} \times \sqrt{7}$) patterns.] Images similar to that in Fig. 7 have also been reported in ref. 8. At higher potentials, E > 1.0 V, where the sulfate coverage is seen to decrease (Fig. 4), the ($\sqrt{3} \times \sqrt{7}$) STM patterns is maintained, indicating that the local (microscopic) sulfate coverage remains fixed. Disordered patches are seen, however, to emerge and eventually envelope the entire surface, removing the ($\sqrt{3} \times \sqrt{7}$) regions in their wake. These changes arise from Au(111) surface oxidation, the oxide thus formed replacing progressively the adsorbed sulfate regions (cf ref. 8).

Adlayer Structural Implications

Magnussen et al have interpreted STM images similar to that in Fig. 7 as indicating the presence of an ordered bisulfate adlayer with a coverage of 0.40, thereby assigning each spot to an adsorbed SO_4 moiety[8]. An apparently attractive structural model considered by Magnussen et al consists of a two-dimensional hydrogen-bound SO_4 adlattice, which resembles closely a compressed solid-state H_2SO_4 structure[8]. However, as already noted, the surface compositional data of Lipkowski et al[9] now indicates ambiguously that the sulfate coverage achieved at the potential where the ordered adlayer forms is only 0.20. [This point can readily be deduced from the chronocoulometric surface-excess data from ref. 9 shown in Fig. 4, which yield $\Gamma_{SO_4} \simeq 2.7 \times 10^{14}$

ions cm^{-2}, corresponding to $\theta_{SO4} \simeq 0.20$ ($\pm$ 0.02) at about 0.8 to 0.9 V.] The present results show that neither the mode of sulfate surface binding nor the adlayer spatial structure, as deduced by IRAS and STM respectively, are changed significantly when electrolyte conditions are altered from those employed in refs. 8 to those in ref. 9. Consequently, we conclude here that the ordered adlayer imaged by STM also corresponds to a sulfate coverage of 0.2, and not 0.4 as suggested in ref. 8. Given that the main tunneling maxima that are reproducibly imaged by STM in the ($\sqrt{3} \times \sqrt{7}$) structure (as in Fig. 6) also correspond to $\theta = 0.2$, it is likely that these features correspond to individual sulfate anions. This real-space structure is shown in ball-model form in Fig. 8, the SO_4 groups being marked as the larger hatched circles, positioned (tentatively) on sites having a net atop symmetry.

While the structural arrangement in Fig. 8 is satisfactory insofar as it is consistent with the surface compositional, IRAS, and STM data, two related (and bothersome) questions remain, which together concoct a more controversial picture of the high-coverage ionic adlayer. Given the strong coulombic repulsions anticipated between nearby adsorbate anions, why is a structure formed which persistently features *nonuniform* ($\sqrt{3}$ and $\sqrt{7}$) interionic distances, especially when alternate ordered arrangements can readily be envisaged which would yield larger and more uniform adsorbate spacings? In addition, what is the physical origin of the "satellite" tunneling maxima seen in some of the STM images?

A direct answer to the second question is problematical, since there are reasons to expect that tunneling maxima in STM adlayer images may arise from electronic structural factors that transcend the mere spatial positions of adsorbate groups[31]. Nevertheless, it is possible that the satellite STM spots arise from hydronium cations which are closely associated with, and perhaps

coadsorbed alongside (or otherwise close to), the sulfate anions. Such cation coadsorption would diminish substantially the coulombic repulsions between adjacent SO_4^{2-} anions, especially along the $\sqrt{3}$ direction, thereby accounting for the non-uniform anion-anion spacing. The approximate positions of the coadsorbed cations as suggested by the STM images, included in the ball model (Fig. 6) as smaller hatched circles, would indeed act to diminish these short-range repulsions and hence stabilize the densely packed ionic adlayer. Evidence for anion-cation coadsorption as imaged by in-situ STM has been obtained recently for another system, iodide/cesium cation adsorption on Au(110), where the intensity of the cation tunneling maxima were also found to be sensitive to the imaging conditions[32].

While this structural model can rationalize well the real-space patterns observed for the ordered adlayer by STM, it faces the difficulty that the inferred equal density of sulfate anions and hydronium cations is formally equivalent to the net adsorption of bisulfate, rather than sulfate, while the latter was concluded to be the predominant adsorbate on thermodynamic grounds[9]. A possible resolution of this apparent conflict may be sought, however, by considering the differing conditions under which the STM and double-layer thermodynamic analyses are carried out. The STM images necessarily refer only to sufficiently high packing densities, indeed corresponding to a saturation coverage in this case, so that the adsorbate is rendered essentially immobile. Given that the sulfate retains part of its anionic charge upon adsorption,* the diminution of coulombic repulsion within the saturated anionic layer brought

---

* A rough estimate of this anionic charge retention can be obtained from the electrosorption valency[33] extracted from the data presented in ref. 9. This value, ca 0.8, is considerably less than that expected, 2, if essentially complete adsorbate-surface charge transfer occurs upon sulfate binding.

about by cation coadsorption may well more than offset the accompanying loss of cation hydration energy. Note that the coadsorbed SO_4^{2-} - H_3O^+ partners may not necessarily form HSO_4^- species, since the propensity for specific H - OSO_3 bond formation will be diminished by sulfate oxygen-gold coordination.

In contrast to the STM data, the electrochemical thermodynamic analysis that is used in ref. 9 to deduce the predominance of sulfate, rather than bisulfate, adsorption in this system refers necessarily to lower (intermediate) sulfate coverages. This is because the analysis exploits the dependence of the adsorbate-induced shift of the electrode potential at a fixed surface electronic charge density, ΔE (σ_m = const), brought about by logarithmic alterations in the sulfate/bisulfate solution concentration, $\ln[SO_4^{2-}]$ or $\ln[HSO_4^-]$[9]. In the particular case where the solution composition is changed by altering the pH for a fixed analytical sulfate concentration, $[SO_4^{2-}]$ and $[HSO_4^-]$ will vary in opposite directions. The sign as well as magnitude of the ΔE (σ_m = const), and hence $\Delta\Gamma_{SO4}$, shifts observed under these conditions therefore enabled Lipkowski et al[9] to deduce the predominant presence of adsorbed SO_4^{2-}. At coverages approaching saturation, however, the ΔE and $\Delta\Gamma_{SO4}$ shifts induced by changes in solution concentrations become very small, hindering and eventually preventing the extraction of information on adsorbate speciation by such thermodynamic means.

Consequently, the thermodynamic data do not eliminate the occurrence of a coadsorbed SO_4^{2-} - H_3O^+ (or related) adlayer at θ_{SO4} = 0.2, although such a situation is precluded at lower sulfate coverages. Another factor to consider, however, is the electrostatic charge distribution in the double layer where the ordered adlayer is formed. From chronocoulometric data of Lipkowski et al[25], in 0.1 M $HClO_4$ + 5 mM K_2SO_4 at 0.90 V vs. SCE, for example (i.e. just beyond the point where the ordered adlayer is formed), the adsorbed sulfate charge $2F\Gamma_{SO4}$

equals $-90.5\ \mu C\ cm^{-2}$ and the electrode charge σ_m is $65\ \mu C\ cm^{-2}$. As noted in ref. 9, such values indicate clearly that sulfate is superequivalently adsorbed and hence that a net cation surface excess Γ_+ is also present so to provide overall electroneutrality.

In a conventional double-layer picture, this cationic charge would be present in the diffuse layer, mostly close to the outer Helmholtz plane. The cation charge would therefore act to screen partly the electrostatic repulsions between the adsorbed sulfate anions. The value of Γ_+ anticipated to be present on this basis, approximately $[-(\sigma_m + 2F\Gamma_{SO4}) = 25.5\ \mu C\ cm^{-2}]$, is somewhat smaller than the cation charge, $F\Gamma_+ = 44.5\ \mu C\ cm^{-2}$, that would reside in the inner layer if the coadsorbed $SO_4^{2-} - H_3O^+$ adlayer model (vide supra) is valid. Consequently, then, if the ordered sulfate adlayer indeed consists of SO_4^{2-}/H_3O^+ pairs the net metal/inner-layer charge $(\sigma_m + 2F\Gamma_{SO4} + F\Gamma_+)$ would be positive, $19\ \mu C\ cm^{-2}$. While certainly not precluded on thermodynamic grounds, such a mixed SO_4^{2-}/H_3O^+ (or HSO_4^- adlayer) would correspond to a net *subequivalent* ionic adsorption, i.e. where the specifically adsorbed charge is insufficient to balance the metal electronic charge. This circumstance would be a non-conventional one, which would probably be viewed with suspicion by many electrochemists.

On the other hand, if the ordered adlayer indeed contains *only* sulfate anions, one is obliged to return to the question of why the observed anion-anion separations in the adlattice are so nonuniform. In the absence of coadsorbed cations, it is plausible that shorter anion-anion distances may be stabilized by specific solvation structures. An interesting prediction of solvent *stabilization* of near-contact anion-anion pairs comes from molecular dynamics and Monte Carlo simulations of Cl^- in water, where nearby anion pairs are predicted to be linked by bridging hydrogen bonding involving water molecules[34,35]. Although there is apparently no direct experimental evidence for such aggregates

either at electrochemical interfaces or in bulk aqueous solution, the possibility of such solvent structured stabilization of ordered ionic adlayers is an intriguing one. It is therefore conceivable that the satellite spots observed in the STM images (Fig. 7) are associated with structured hydration rather than hydronium cations, even though there is no persuasive reason to prefer either of these aqueous structural models at the present time.

It is nonetheless worth commenting further on the present IRAS results in this context. As noted above, the occurrence of the sulfate disorder-order transition, so to yield the ($\sqrt{3} \times \sqrt{7}$) adlayer, is accompanied by only minor (ca 5 cm^{-1}) downshifts in the ν_{SO} frequency. This finding suggests that the coordination environment of the adsorbed sulfate is altered only slightly by the occurrence of the phase transition. Indeed, the observed small ν_{SO} frequency downshift upon adlayer ordering is not inconsistent with a slight weakening of S-O bands incurred by hydrogen bonding with juxtaposed water molecules. On the other hand, the IRAS results certainly do not eliminate the possibility that adjacent SO_4^{2-} - H_3O^+ pairs are present in the ordered adlayer. While the formation of such pairs (and especially HSO_4^-) would be expected to incur greater changes in the ν_{SO} bands, hydronium ion coadsorption may be initiated at potentials below the disorder-order transition, so that the hydronium surface excess and hence the local environment surrounding the adsorbed sulfate does not incur a *discontinuous* change when adlayer ordering occurs. Harmoniously, there is no significant discontinuity in the sulfate surface excess at this point (Fig. 4)[9].

The reader may therefore conclude, not unfairly, that the present intercomparison between IRAS, STM, and thermodynamic surface compositional data for the Au(111)/sulfate system raises at least as many (unsettling!) questions as it provides answers. It is certainly apparent that a more clearcut resolution

of the (surprising) structure of the ordered sulfate adlayer will require independent experimental evidence from other microscopic structural probes, such as X-ray scattering. However, an inherent value of intercomparing such structural and spectroscopic data, as offered here by STM and IRAS, lies in the link provided by the latter measurements between the ordered structures, accessed by the former technique, to lower coverage states for which directed surface bonding may well still occur yet interadsorbate disorder prevails. The ordered, high-coverage, adsorbate regime may well contain many structural surprises, not only in view of our new-found ability to scrutinize such adlayers at the atomic/molecular level but also because the solute surface concentrations and charge densities are higher than those considered in traditional models of the electrochemical double layer. Evidently, then, such comparisons should contribute increasingly to our developing understanding of the interplay between structure and bonding energetics within ionic electrochemical adlayers.

ACKNOWLEDGMENTS

We are grateful to Professors Jacek Lipkowski and Andrzej Wieckowski for sharing ref. 9 prior to publication and for helpful comments, and also to the former for generously supplying additional chronocoulometric data. We are also indebted to Dr. Antoinette Hamelin for preparing the Au(111) crystal. This work is supported by the Office of Naval Research and the National Science Foundation.

References

1) M.J. Weaver and X. Gao, Ann. Rev. Phys. Chem., 44 (1993), 459.

2) X. Gao and M.J. Weaver, Ber. Bunsenges. Phys. Chem., 97 (1993), 507.

3) M.F. Toney and O.R. Melroy, in "Electrochemical Interfaces", H.D. Abruña, ed., VCH Publishers, New York, 1991, Chapter 2.

4) S-L. Yau, X. Gao, S-C. Chang, B.C. Schardt, and M.J. Weaver, J. Am. Chem. Soc., 113 (1991), 6049.

5) X. Gao, S-C. Chang, X. Jiang, A. Hamelin, and M.J. Weaver, J. Vac. Sci. Tech., A10 (1992), 2972.

6) I. Villegas and M.J. Weaver, in preparation.

7) C. Stuhlmann, I. Villegas, and M.J. Weaver, Chem. Phys. Lett., submitted.

8) O.M. Magnussen, J. Hageböck, J. Hotlos, and R.J. Behm, Far. Disc., 94 (1992), 329; also see discussion on pp. 398–400.

9) Z. Shi, J. Lipkowski, M. Gamboa, P. Zelenay, and A. Wieckowski, J. Electroanal. Chem., in press.

10) K. Kunimatsu, M.G. Samant, and H. Seki, J. Electroanal. Chem., 258 (1989), 163; 272 (1989), 185.

11) M.G. Samant, K. Kunimatsu, H. Seki, and M.R. Philpott, J. Electroanal. Chem., 280 (1990), 391.

12) P.W. Faguy, N. Markovic, R.R. Adzic, C.A. Fierro, and E.B. Yeager, J. Electroanal. Chem., 289 (1990), 245.

13) R.J. Nichols, in "Adsorption of Molecules at Metal Electrodes", J. Lipkowski and P.N. Ross, eds., VCH Publishers, New York, 1992, Chapter 7.

14) F.C. Nart and T. Iwasita, J. Electroanal. Chem., 308 (1991), 277.

15) F.C. Nart and T. Iwasita, J. Electroanal. Chem., 322 (1992), 289.

16) V.B. Paulissen and C. Korzeniewski, J. Electroanal. Chem., 351 (1993), 329.

17) P.W. Faguy, N. Markovic, and P.N. Ross, J. Electrochem. Soc., 140 (1993), 1638.

18) H. Ogasawara, Y. Sawatari, J. Inukai, and M. Ito, J. Electroanal. Chem., 358 (1993), 337.

19) D.B. Parry, M.G. Samant, H. Seki, M.R.Philpott, and K. Ashley, Langmuir, 9 (1993), 1878.

20) D.S. Corrigan and M.J. Weaver, J. Phys. Chem., 90 (1986), 5300.

21) S-C. Chang and M.J. Weaver, J. Chem. Phys., 92 (1990), 4582.

22) X. Gao, A. Hamelin, and M.J. Weaver, Phys. Rev. Lett., 67 (1991), 618.

23) X. Gao, G.J. Edens, A. Hamelin, and M.J. Weaver, Surf. Sci., 296 (1993), 333.

24) D.S. Corrigan, E.K. Krauskopf, L.M. Rice, A. Wieckowski, and M.J. Weaver, J. Phys. Chem., 92 (1988), 1596.

25) J. Lipkowski, personal communication.

26) D.S. Corrigan and M.J. Weaver, J. Electroanal. Chem., 239 (1988), 55.

27) J.D. Roth and M.J. Weaver, Anal. Chem., 63 (1991), 1603.

28) K. Kunimatsu, M.G. Samant, H. Seki, and M.R. Philpott, J. Electroanal. Chem., 243 (1988), 203.

29) X. Gao and M.J. Weaver, J. Am. Chem. Soc., 114 (1992), 8544.

30) K. Nakamoto, in "Infrared and Raman Spectra of Inorganic and Coordination Compounds", Wiley, New York, 1986, p. 248-51.

31) J. Wintterlin and R.J. Behm, in "Scanning Tunneling Microscopy I", Springer Series in Surface Sciences, Vol. 20, H-J. Güntherodt and R. Wiesendanger, eds., Springer-Verlag, Berlin, 1992. Chapter 4.

32) X. Gao and M.J. Weaver, in preparation.

33) K.J. Vetter and J.W. Schultze, J. Electroanal. Chem., 44 (1973), 63; 53 (1974), 67.

34) L.X. Dang and B.M. Pettitt, J. Phys. Chem., 94 (1990), 4304.

35) J.K. Buckner and W.L. Jorgensen, J. Am. Chem. Soc., 111 (1989), 2507.

FIGURE CAPTIONS

Figure 1

Cyclic voltammogram at 50 mV s^{-1} for Au(111) in 0.1 M $HClO_4$ + 5 mM H_2SO_4 (solid trace) and 0.1 M H_2SO_4 (dashed trace) in IRAS thin layer.

Figure 2

Series of potential-difference infrared (PDIR) spectra on Au(111) in (A) 0.1 M $HClO_4$ + 5 mM H_2SO_4 and (B) 0.1 M H_2SO_4. Lower (reference) potential was 0 V vs. SCE; upper sample potentials as indicated. Potential was altered after every 32 interferometer scans, a total of 256 scans at both reference and sample potentials being acquired.

Figure 3

Plot of peak frequency, ν_{SO}, for adsorbed sulfate on Au(111) in 0.1 M $HClO_4$ + 5 mM H_2SO_4 versus electrode potential. Infrared spectra obtained as in Fig. 2A.

Figure 4

Integrated intensities of ν_{SO} band, A_1, for sulfate on Au(111) in 0.1 M $HClO_4$ + 5 mM H_2SO_4 versus electrode potential, E (filled circles), compared with sulfate surface excess, Γ_{SO4}, in 0.1 M $HClO_4$ + 5 mM K_2SO_4 obtained by chronocoulometry[9,25] (open circles) and Γ_{SO4} values in 0.1 M $HClO_4$ + 0.5 mM K_2SO_4 obtained by radiotracer measurements[9] (open triangles).

Figure 5

PDIR spectra on Au(111) in 0.5 M H_2SO_4 (lower) and in 0.1 M Na_2SO_4 + 1 mM H_2SO_4 (upper). The sample and reference potentials were 0.75 and 0 V in both cases.

Figure 6

Constant-height STM image for Au(111) in 0.1 M $HClO_4$ + 5 mM H_2SO_4. Image was upward-rastered, the electrode potential being stepped from 0.5 V to 0.9 V one-third up the image as shown. Tunneling current = 10 nA; tip-surface bias voltage = -0.5 V.

Figure 7

Height-shaded STM image for Au(111) in 0.1 M H_2SO_4, obtained at 0.9 V. Tunneling current = 10 nA; tip-surface bias voltage = -0.07 V.

Figure 8

Proposed real-space structure of Au(111)/SO_4^{2-} adlayer. Larger hatched circles refer to sulfate anions, and smaller hatched circles to possible coadsorbed cations or oriented hydration (see text).

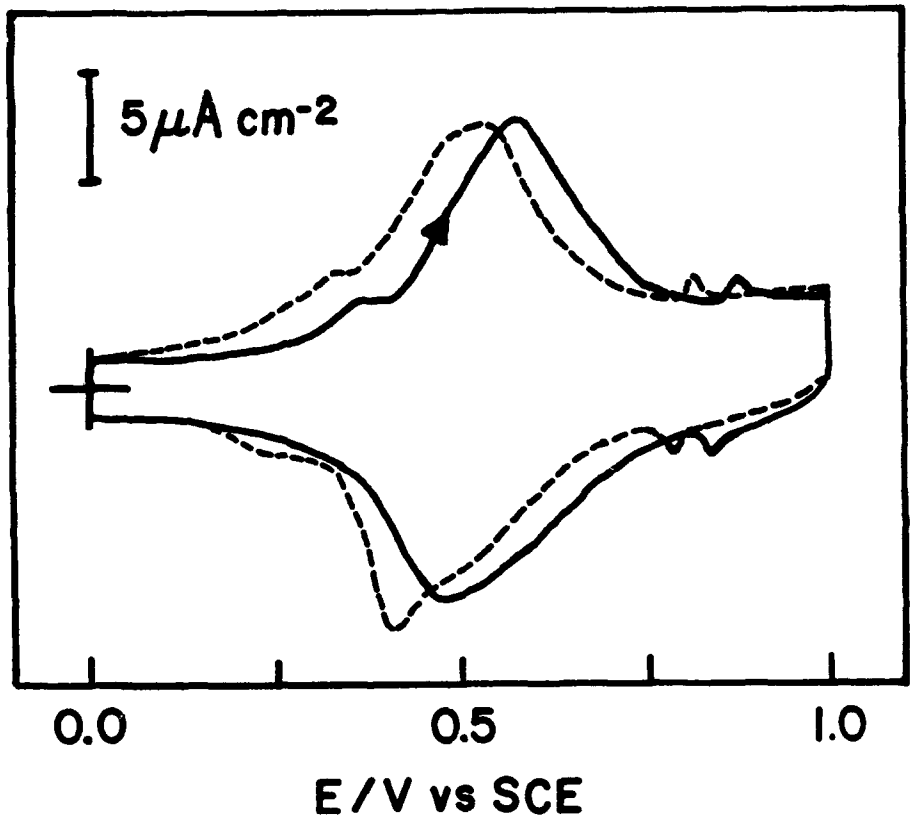
5μA cm⁻²
0.0
0.5
1.0
E/V vs SCE

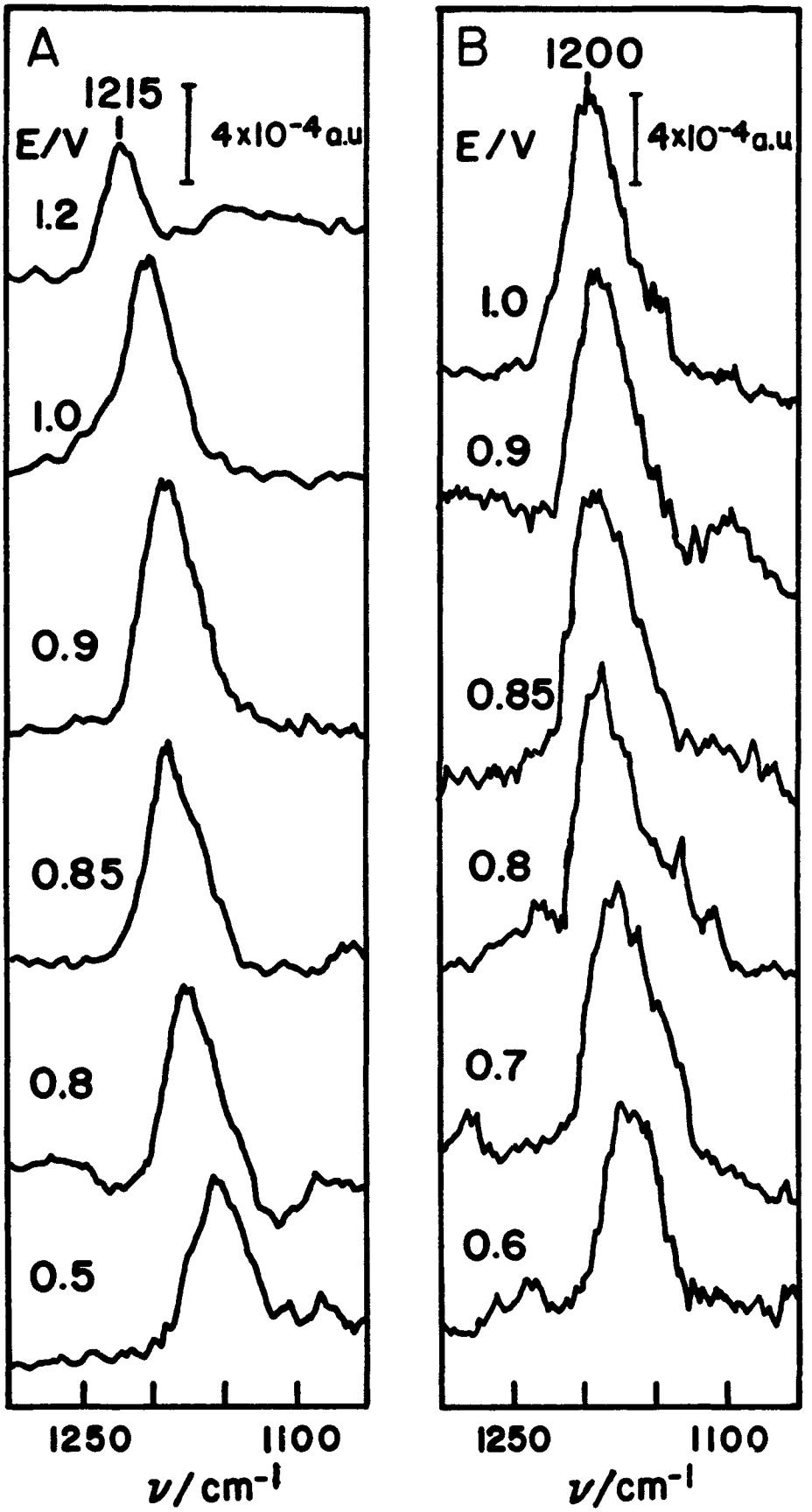
A
1215
E/V
4x10⁻⁴a.u
1.2
1.0
0.9
0.85
0.8
0.5
1250
1100
ν/cm⁻¹
B
1200
E/V
4x10⁻⁴a.u
1.0
0.9
0.85
0.8
0.7
0.6
1250
1100
ν/cm⁻¹

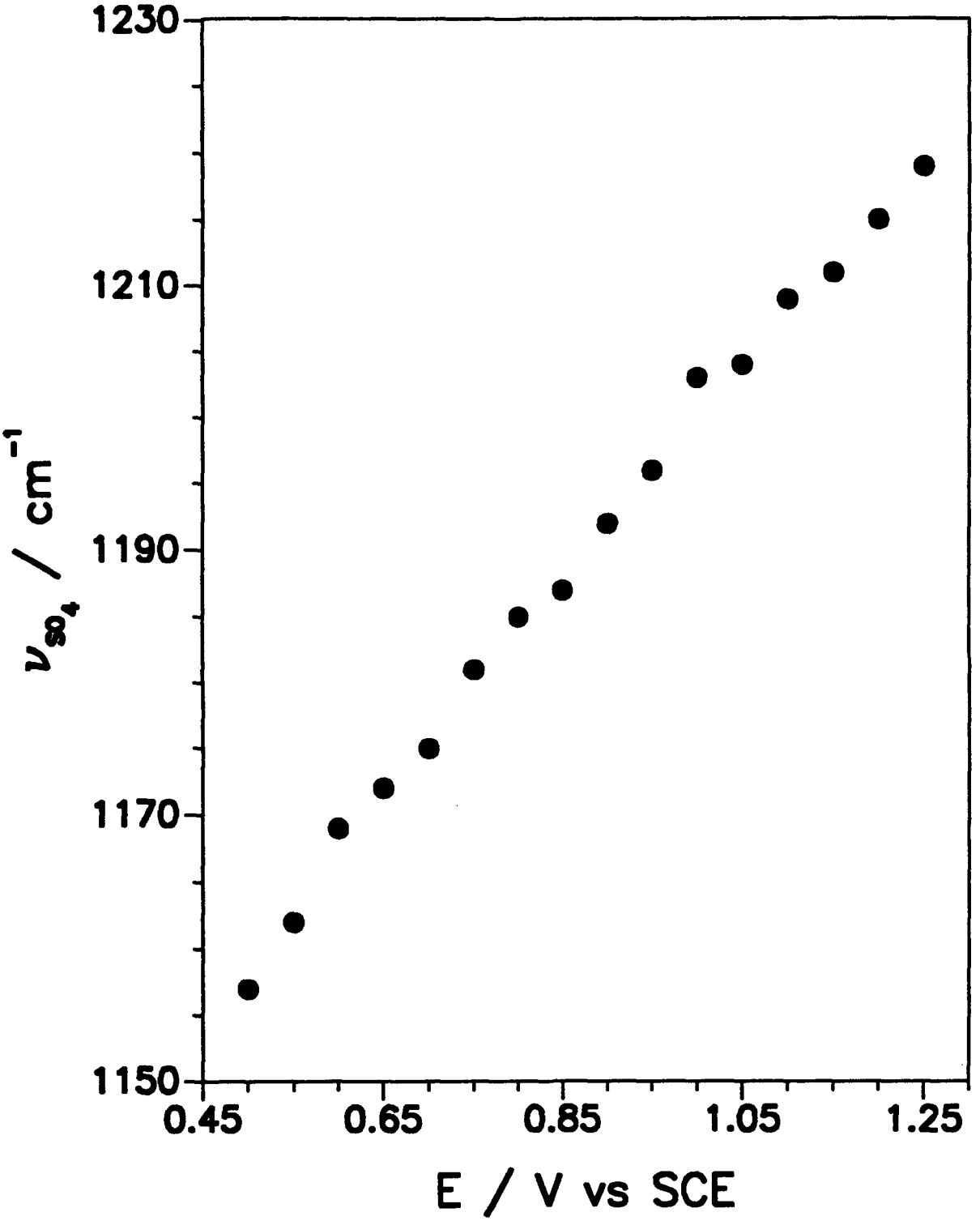
1230
1210
1190
1170
1150
ν_{SO_4} / cm^{-1}
0.45
0.65
0.85
1.05
1.25
E / V vs SCE

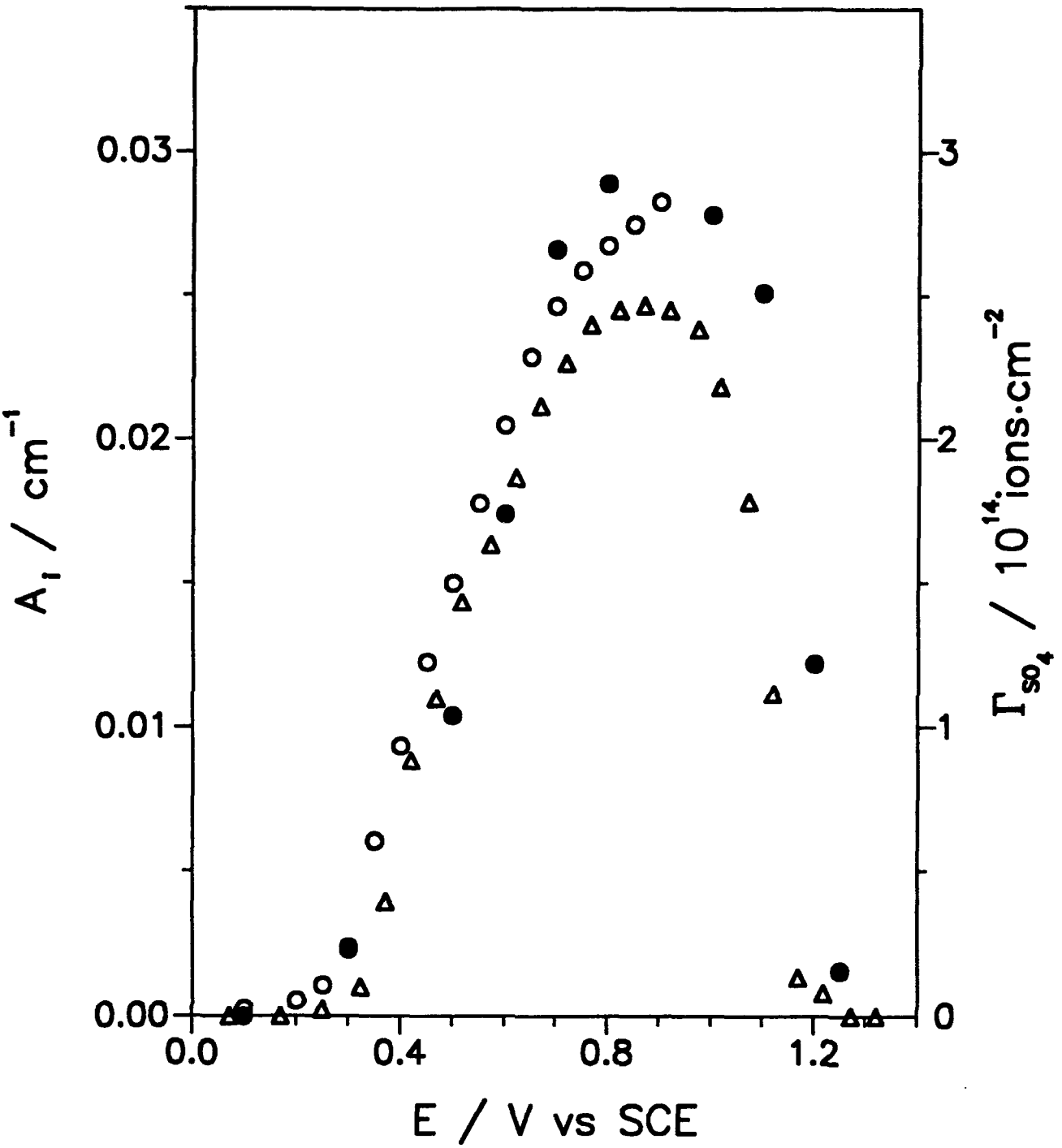
0.03
0.02
0.01
0.00
3
2
1
0
0.0
0.4
0.8
1.2
E / V vs SCE
A_1 / cm^{-1}
Γ_{SO_4} / 10^{14} ions·cm^{-2}

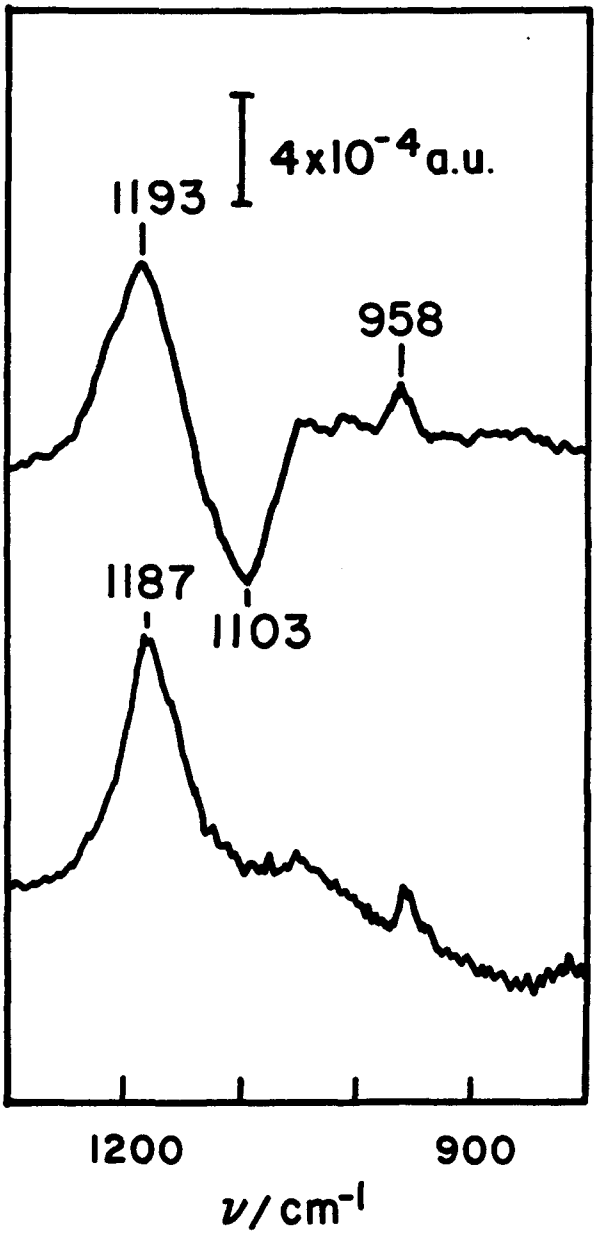
4x10⁻⁴a.u.
1193
958
1187
1103
1200
900
ν/cm⁻¹

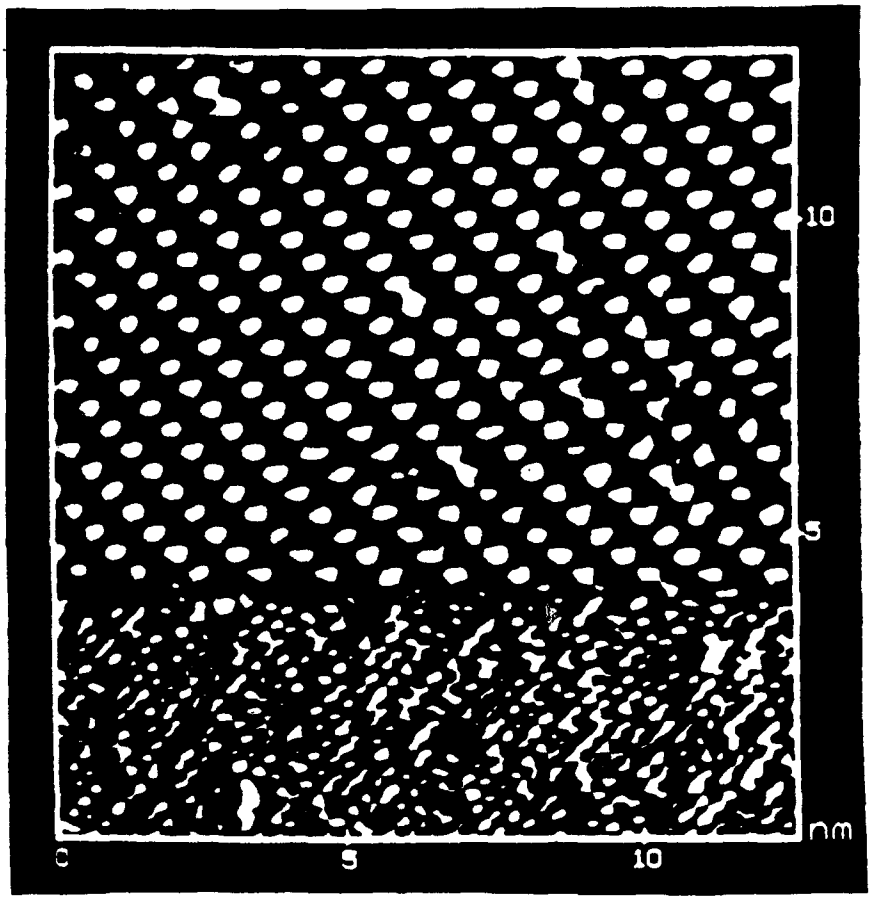
10
5
nm
0
5
10

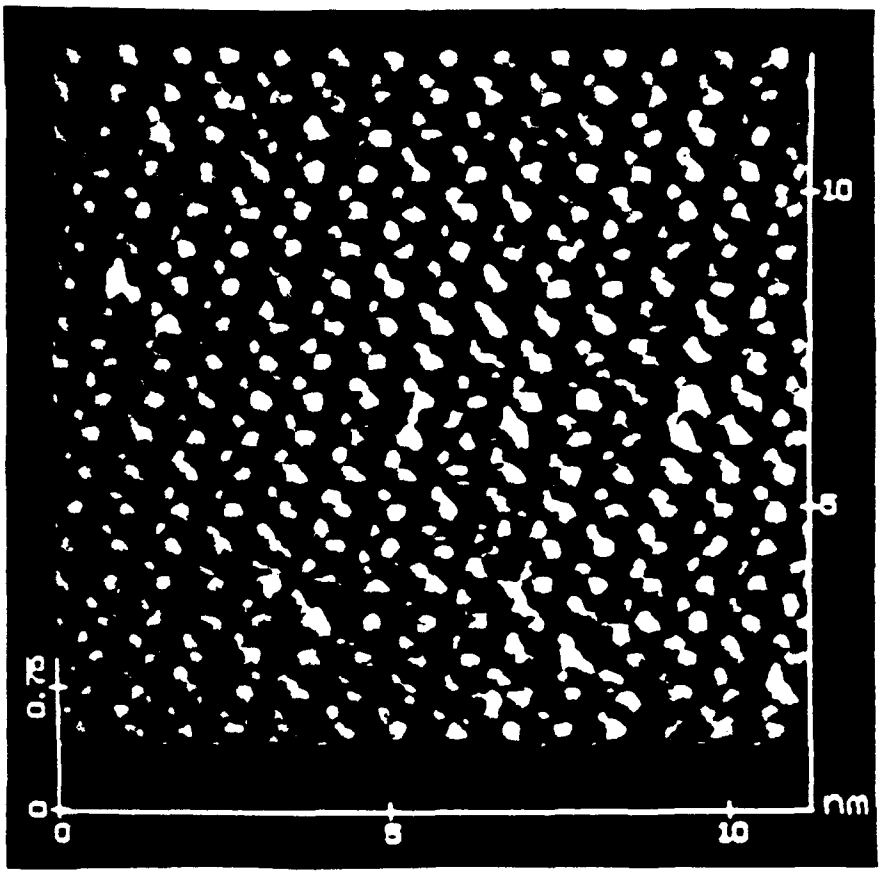
0
0.75
0
5
10
nm
10
5

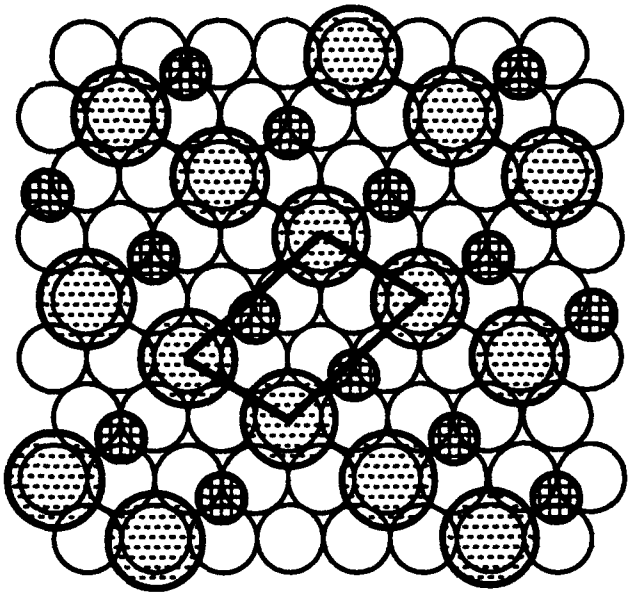

Au(111)-SO_4 ($\sqrt{3}$x$\sqrt{7}$)